

Supplementary Information

Magneto-plasmonic bionanocomposites for on site SERS detection of water contaminants

Sofia F. Soares¹, Nuno M. A. S. Silva¹, João Brenheiro¹, Sara Fateixa¹, Ana L. Daniel-da-Silva¹ and Tito Trindade^{1*}

¹CICECO-Aveiro Institute of Materials and Department of Chemistry, University of Aveiro, 3810-193 Aveiro, Portugal

A. Calibration curves

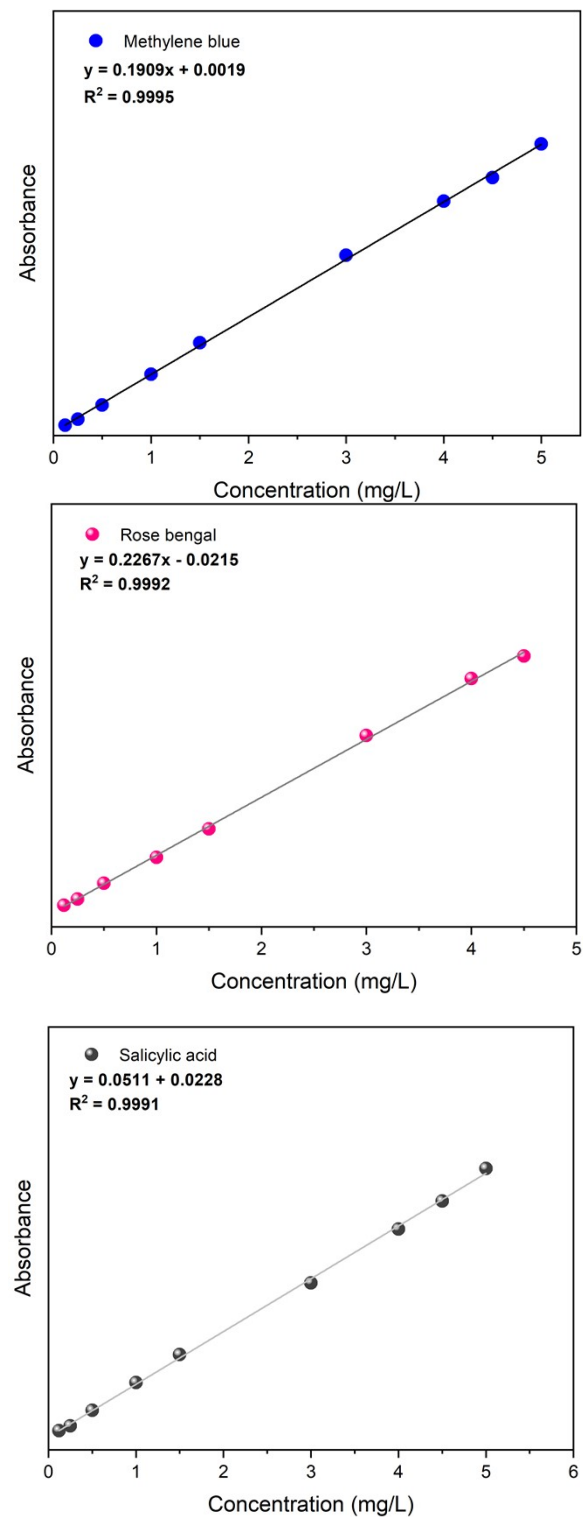


Fig. S1.
Calibration

curves for methylene blue, rose bengal and salicylic acid in ultra-pure water, obtained by UV-VIS spectroscopy.

B. Materials characterization

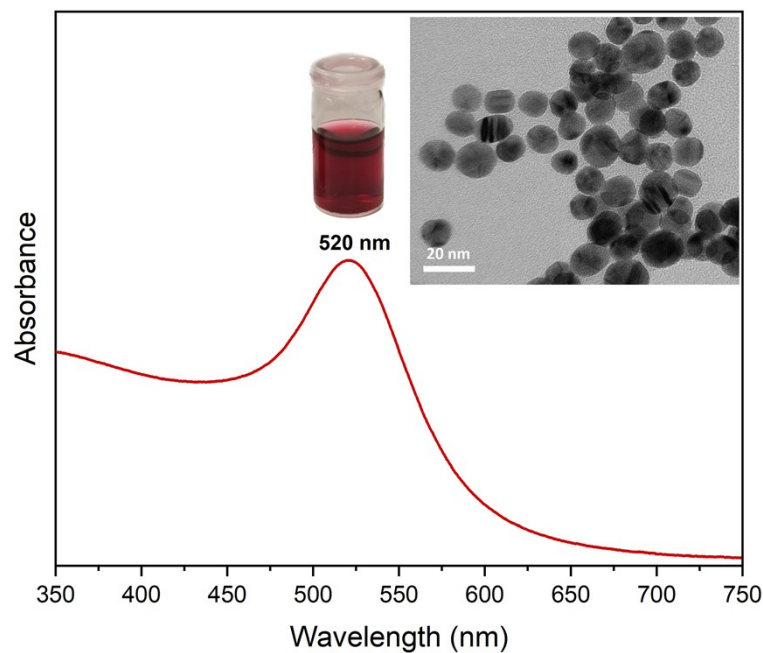


Fig. S2. UV-VIS absorption spectrum of colloidal Au nanoparticles. Inset: photograph of the Au colloid and TEM image of gold nanoparticles.

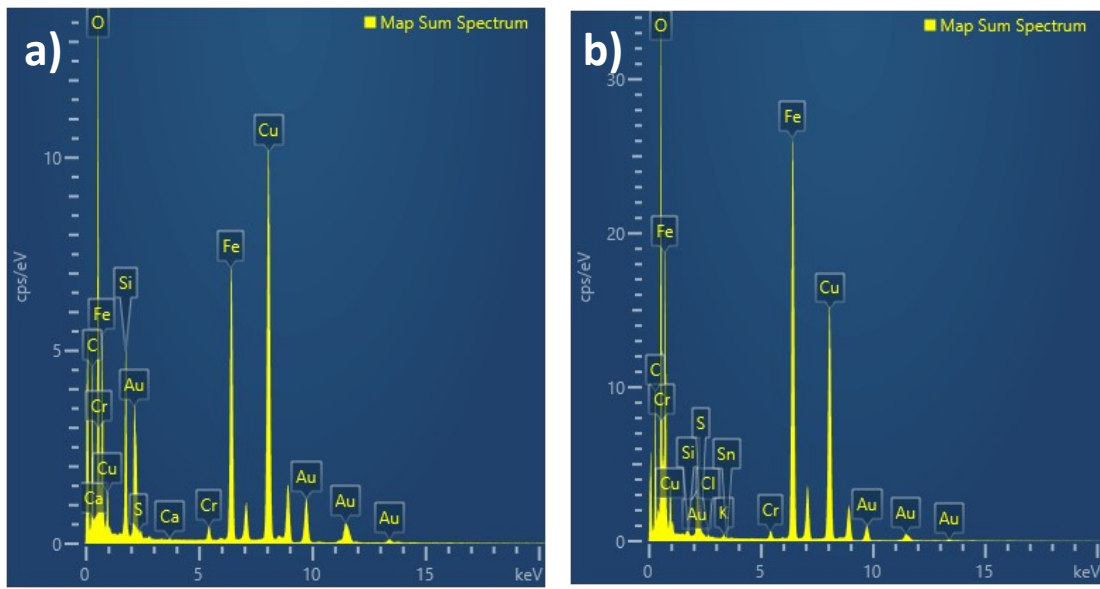


Fig. S3. EDS spectra of a) $\text{Fe}_3\text{O}_4@\text{SiO}_2/\text{SiTMC}/\text{Au}_{\text{ex situ}}$ and b) $\text{Fe}_3\text{O}_4@\text{SiO}_2/\text{SiTMC}/\text{Au}_{\text{in situ}}$ nanocomposites.

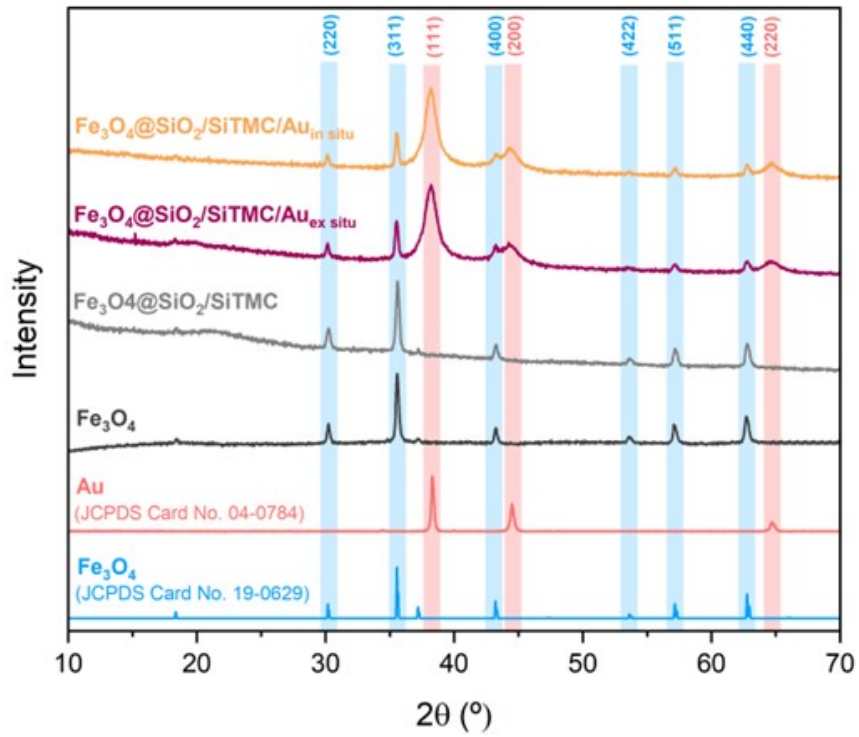


Fig. S4. XRD diffraction patterns of the synthesized materials: Fe_3O_4 , $\text{Fe}_3\text{O}_4@\text{SiO}_2/\text{SiTMC}$, $\text{Fe}_3\text{O}_4@\text{SiO}_2/\text{SiTMC}/\text{Au}_{\text{ex situ}}$ and $\text{Fe}_3\text{O}_4@\text{SiO}_2/\text{SiTMC}/\text{Au}_{\text{in situ}}$ nanocomposites. For comparison purposes, reported diffractograms for crystalline gold with face centered structure (JCPDS Card No. 04-0784) and Fe_3O_4 (JCPDS Card No. 19-0629) were also included.

C. Dyes adsorption

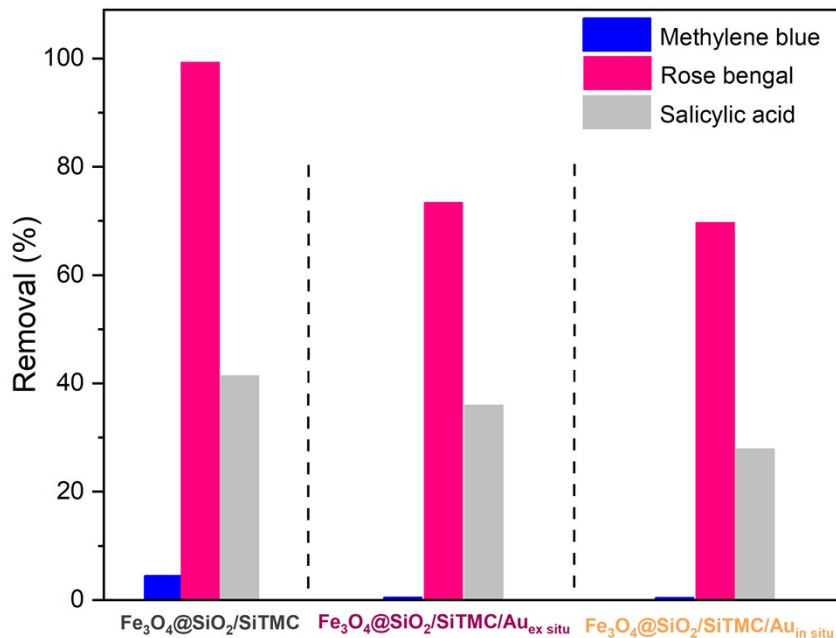


Fig. S5. Removal percentage of methylene blue, rose bengal and salicylic acid using $\text{Fe}_3\text{O}_4@\text{SiO}_2/\text{SiTMC}$, $\text{Fe}_3\text{O}_4@\text{SiO}_2/\text{SiTMC}/\text{Au}_{\text{ex situ}}$ and $\text{Fe}_3\text{O}_4@\text{SiO}_2/\text{SiTMC}/\text{Au}_{\text{in situ}}$ particles (Conditions: adsorbent dose of 0.5 mg/mL, 4 h of contact time, initial concentration of 1×10^{-5} M, 5×10^{-5} M and 1×10^{-3} M for methylene blue, rose bengal and salicylic acid respectively).

D. SERS

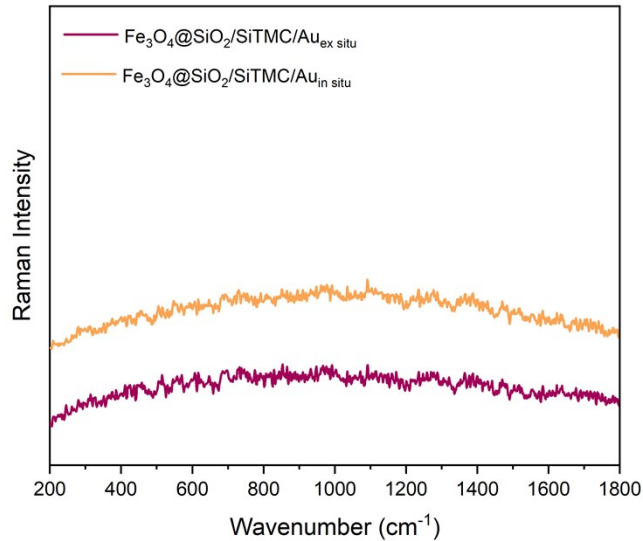


Fig. S6. Conventional Raman spectra of $\text{Fe}_3\text{O}_4@\text{SiO}_2/\text{SiTMC}/\text{Au}_{\text{ex situ}}$ and $\text{Fe}_3\text{O}_4@\text{SiO}_2/\text{SiTMC}/\text{Au}_{\text{in situ}}$ nanocomposites, under 633 nm laser excitation.

Table S1: Experimental Raman band positions (wavenumber, cm^{-1}) for methylene blue (MB)^{1,2}, rose bengal (RB)^{3,4} and salicylic acid (SA)^{5,6} with the corresponding vibrational mode assignments.

Wavenumber (cm^{-1})	Vibrational modes
MB	
1621	$\nu(\text{CC}) + \delta_{\text{in-plane}}(\text{CH})$ (ring), $\nu(\text{CN}) + \nu(\text{CC})$
1430	$\delta_{\text{out-plane}}(\text{CH})$, $\delta(\text{CH}_3)$, $\nu(\text{CC})$, $\nu_{\text{sym}}(\text{CN})$
1396	$\nu_{\text{sym}}(\text{CN})$ (lateral and centre) + $\delta_{\text{in-plane}}(\text{CH})$ (ring) + $\delta_{\text{out-plane}}(\text{CH})$, $\delta(\text{CH}_3)$, $\nu(\text{CN}) + \nu(\text{CC})$, $\nu_{\text{asym}}(\text{CN})$
1181	$\delta_{\text{in-plane}}(\text{CH})$ (ring) + $\delta_{\text{out-plane}}(\text{CH})$, $\delta(\text{CH}_3)$, $\delta_{\text{in-plane}}(\text{CH})$
480	$\delta_{\text{in-plane}}$ thiazine (ring)
448	Skeletal deformation (CN, CS and CH_3), CN skeletal deformation
RB	
1619	$\nu_{\text{sym}}(\text{C=C})$ (ring)
1488	$\nu_{\text{asym}}(\text{C=C})$ (ring)
1297	$\delta(\text{CCC})$ (ring) + $\delta(\text{C-H})$
614	$\nu(\text{C-I}) + \delta(\text{CCO})$
SA	
1625	$\nu(\text{C=O})$
1583	$\nu_{\text{asym}}(\text{OCO})$

1390	$\nu_{\text{sym}}(\text{OCO})$
1353	$\delta(\text{C}_{\text{ring}}\text{-OH})$
1255	$\nu(\text{C}_{\text{ring}}\text{-OH})$

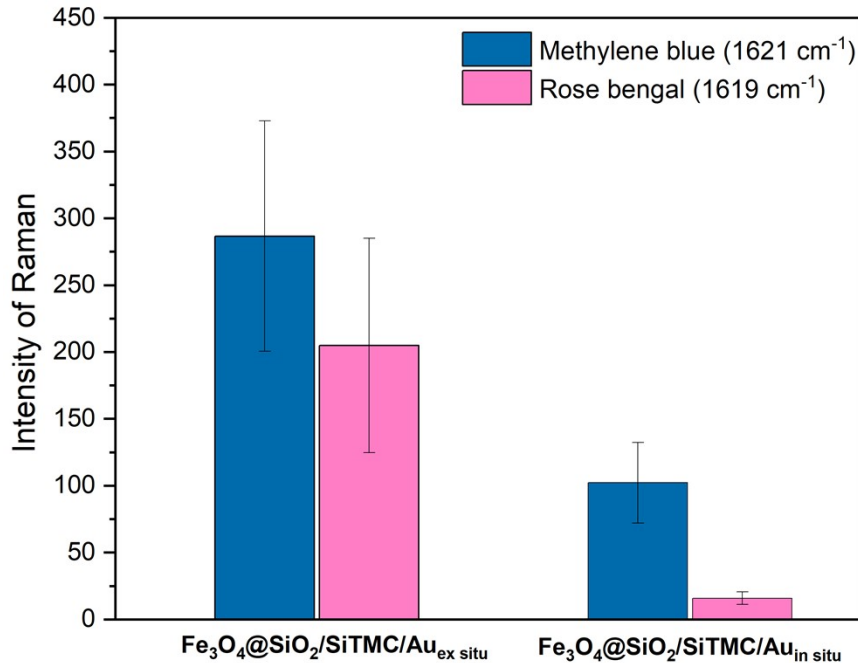


Fig. S7. Plot of the Raman intensities of selected vibrational bands of MB and RB, for comparing the SERS performance of the $\text{Fe}_3\text{O}_4@\text{SiO}_2/\text{SiTMC}/\text{Au}_{\text{ex situ}}$ and $\text{Fe}_3\text{O}_4@\text{SiO}_2/\text{SiTMC}/\text{Au}_{\text{in situ}}$ bionanocomposites (data from 5 random Raman spectra).

References

- 1 S. Fateixa, M. Wilhelm, H. I. S. Nogueira and T. Trindade, *Journal of Raman Spectroscopy*, 2016, **47**, 1239–1246.
- 2 G.-N. Xiao and S.-Q. Man, *Chem Phys Lett*, 2007, **447**, 305–309.
- 3 Y. Xia, P. Padmanabhan, S. Sarangapani, B. Gulyás and M. Vadakke Matham, *Sci Rep*, 2019, **9**, 8497.
- 4 A. M. Gabudean, M. Focsan and S. Astilean, *The Journal of Physical Chemistry C*, 2012, **116**, 12240–12249.
- 5 J. L. Castro, J. F. Arenas, M. R. López-Ramírez, D. Peláez and J. C. Otero, *J Colloid Interface Sci*, 2009, **332**, 130–135.

- 6 S. Adomavičiūtė-Grabusovė, S. Ramanavičius, A. Popov, V. Šablinskas, O. Gogotsi and A. Ramanavičius, *Chemosensors*, 2021, **9**, 223.